

GaAs MESFET Regenerator for Phase-Shift Keying Signals at the Carrier Frequency

SHOZO KOMAKI, OSAMU KURITA, AND TADASHI MEMITA

Abstract—This paper describes a GaAs metal-semiconductor FET (GaAs MESFET) phase regenerator for biphasic phase-shift keying (PSK) signals at the carrier frequency. By using this regenerator, decision and reshaping of the signals can be made without detection, thus repeaters can be simplified. This paper shows that phase regeneration is characterized by the symbol m , which denotes the ratio of the normal signal to the phase-inverted signal. Ideal phase regeneration is obtained for $m = 1$. An analysis of the ratio m for the MESFET regenerator is presented, and it is shown that, if the gate bias or the local-oscillator power level are selected at a slightly higher point than that minimizing the conversion loss, then $m = 1.03$ is obtained at an excess loss of 3 dB. To verify this analysis, the ratio m was measured experimentally and it was found to agree with the analysis. Static and dynamic characteristics were also measured, and it is shown that the MESFET regenerator has decision and reshaping ability.

I. INTRODUCTION

A digital-transmission system at microwave frequencies was recently developed and is planned to be implemented. The number of relay stations in such a system must be increased in order to reduce rainfall attenuation. For this reason, it is necessary to reduce the cost and size of the repeaters. A hybrid system, consisting of several linear-repeater stations and a regenerative station, can be one of the solutions to this problem. In place of the linear repeater, a "direct regenerator," which directly regenerates phase-shift keying (PSK) signals at the carrier frequency, can be used for the hybrid system. Because the direct regenerator can discriminate and reshape the signals without detection, no detector or modulator are required for the repeater. Hence, the direct regenerator can reduce the cost and size compared with the regenerative repeater. Furthermore, it is superior to the linear amplifier in noise-suppression characteristics.

The direct regenerators reported so far used the tunnel-diode parametric amplifier [1]–[4]. In such regenerators, a circulator is unavoidable in order to separate the input and the output ports. This paper proposes a direct regenerator with the GaAs metal-semiconductor FET (GaAs MESFET), resulting in easy separation of the input from the output port.

Section II describes the principle of operation using a block diagram of the direct regenerator. As a result, it is shown that the effect of phase regeneration can be characterized by the symbol m , which denotes the ratio of the normal signal to the phase inverted signal. Section III reports on a detailed investigation of the MESFET phase regenerator and

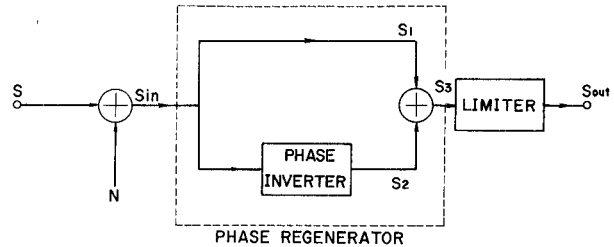


Fig. 1. Typical block diagram of the direct regenerator.

on the calculation of the ratio m . The final part, Section IV, describes the measured static and dynamic characteristics.

The MESFET regenerator described here is believed to open a new field for various MESFET circuits in communication systems.

II. PRINCIPLE OF REGENERATION

Fig. 1 shows a typical block diagram of the direct regenerator, where the phase inverter inverts the phase ϕ of the input signal into the negative phase $-\phi$ at the output signal S_2 . The phase ϕ of the input signal is defined with respect to an unmodulated noiseless carrier.¹ The summing circuit \oplus operates such that $S_3 = S_1 + S_2$, as shown in Fig. 1. The limiter suppresses the amplitude fluctuations of the signal S_3 . The binary phase-modulated signal S at the input of the receiver is distorted by additive noise N . The input signal of the direct regenerator is, therefore, the summation of S and N , i.e.,

$$\begin{aligned} S_{in} &= S + N \\ &= A \cos(\omega t + \phi(t)) \end{aligned} \quad (1)$$

where A and $\phi(t)$ are the amplitude and phase of the input signal, respectively, and ω is the angular frequency of the carrier. As shown in Fig. 1, S_{in} is divided into two components. One component is fed into the phase inverter. The output signal S_2 of the phase inverter is written as

$$S_2 = B_2 \cos(\omega t - \phi(t)) \quad (2)$$

where B_2 is the amplitude of the inverter's output signal S_2 . The other signal component S_1 , which can be written as

$$S_1 = B_1 \cos(\omega t + \phi(t)) \quad (3)$$

where B_1 is the amplitude of S_1 , is fed directly into a summing circuit and summed with S_2 . Thus the output signal

¹ In an actual repeater, this carrier has to be generated. This can be accomplished with several standard techniques.

Manuscript received September 23, 1975; revised December 12, 1975.

The authors are with the Electrical Communication Laboratory, Nippon Telegraph and Telephone Public Corporation, Yokosuka-shi, Kanagawa-ken, 238-03 Japan.

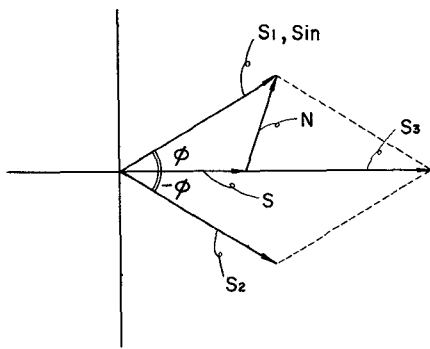


Fig. 2. Direct regenerator phasor diagram.

S_3 of the summing circuit is given by

$$\begin{aligned} S_3 &= S_1 + S_2 \\ &= B_1 \cos(\omega t + \phi(t)) + B_2 \cos(\omega t - \phi(t)). \quad (4) \end{aligned}$$

For

$$B_1 = B_2 \quad (5)$$

as illustrated in Fig. 2, (4) becomes

$$\begin{aligned} S_3 &= B_1(\cos(\omega t + \phi(t)) + \cos(\omega t - \phi(t))) \\ &= 2B_1 \cos \phi(t) \cos(\omega t) \\ &= 2B_1 |\cos \phi(t)| \cos(\omega t + \psi(t)) \quad (6) \end{aligned}$$

where

$$\psi(t) = \begin{cases} 0, & -\pi/2 \leq \phi \leq \pi/2 \\ \pi, & -\pi < \phi < -\pi/2, \quad \pi/2 < \phi < \pi. \end{cases} \quad (7)$$

Since S_3 is fed into a limiter, its output signal can be written as

$$S_{\text{out}} = C \cos(\omega t + \psi(t)). \quad (8)$$

It is shown, from (8), that 1) the output signal of this direct regenerator has neither amplitude nor phase fluctuations; and 2) the input signal is phase discriminated by the decision limit of $\pm \pi/2$. Conditions 1) and 2) are the necessary and satisfactory conditions for binary phase regeneration.

On the other hand, if (5) is not satisfied, the ratio m , which is defined as

$$m = B_1/B_2 \quad (9)$$

is not unity. In this case, the phase of S_3 , equivalent to the phase of S_{out} , is as shown in Fig. 3. This figure shows that: 1) For $m = 1$, the phase characteristic is step-like, and phase regeneration is ideal. 2) As the ratio m increases or decreases from unity, the phase regeneration becomes less and less effective, and, in the case of $m = 0$ or ∞ , phase regeneration becomes impossible. 3) For $0.95 \leq m \leq 1.05$, almost perfect regeneration can be expected.

Fig. 4 shows the amplitude of the signal S_3 normalized to $B_1 + B_2$. This figure shows that fluctuations of the input phase ϕ cause fluctuations of the output amplitude $|S_3|$. The limiter is thus necessary to suppress amplitude fluctuations. When $m = 1$, the amplitude decreases with $\cos \phi(t)$, as is evident from (6).

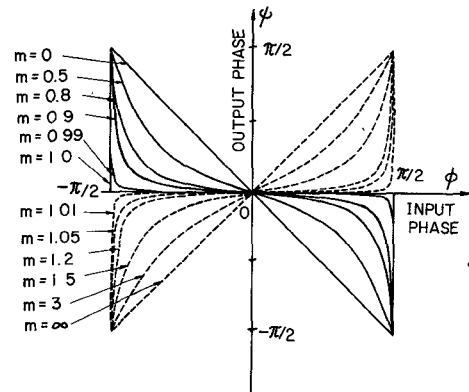


Fig. 3. Phase-regenerator input-output phase characteristics.

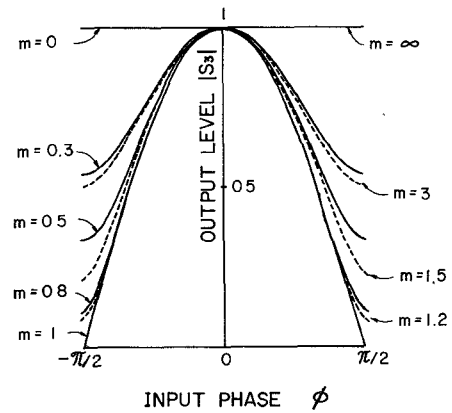


Fig. 4. Phase-regenerator amplitude characteristics.

III. MESFET PHASE-REGENERATION CHARACTERISTICS

This section describes a MESFET mixer required in the phase regenerator. Fig. 5 shows a possible realization of the mixer. The frequency of the local oscillator is twice that of the input signal. The local-oscillator signal can easily be generated by a doubler followed by a narrow-band filter or other techniques [2]–[4]. At the Schottky gate the local-oscillator signal is mixed with the input signal. The mixed signal has the same frequency and the inverse phase as the input signal, i.e.,

$$\cos(2\omega t - (\omega t + \phi)) = \cos(\omega t - \phi). \quad (10)$$

The mixed signal and the input signal voltage are both imposed on the gate conductance, are amplified, and the output is finally extracted from the drain port. If the amplitudes of these signals are equal, then the ratio m is unity, and the output signal of the MESFET mixer is ideally regenerated in phase. In this manner, the MESFET mixer functions as a phase regenerator with amplification.

An equivalent circuit of the MESFET is shown in Fig. 6. In general, the source resistance R_s is much smaller than the drain resistance $1/G_D$, ($R_s \ll 1/G_D$), so the feedback effect by R_s can be neglected. If this effect is neglected, the MESFET mixer can be analyzed using general mixer theory [5]. The equivalent circuit for the mixing port, which is the gate, is shown in Fig. 7. In the MESFET, mixing is performed not only by variations in g but also by variations in C . How-

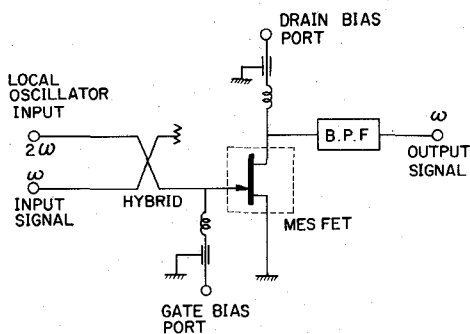


Fig. 5. Circuit diagram of the MESFET phase regenerator.

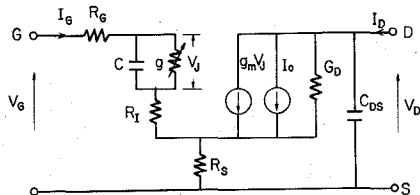
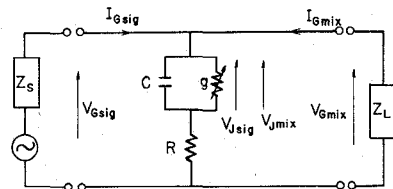
Fig. 6. Equivalent circuit of the MESFET phase regenerator. ($R = R_G + R_I + R_s = 50 \Omega$; $C = 0.5 \text{ pF}$; $\alpha = 18.5$; $g_m = 15 \text{ mV}$; $G_D = 2.0 \text{ m}\Omega$; $I_S = 1 \text{ pA}$).

Fig. 7. Equivalent circuit for the mixing port.

ever, the capacitance variations are neglected to simplify the analysis. In this figure, it is assumed that the image signal is short circuited, and that conversion-conductance terms higher than second order are neglected. The load impedance Z_L is determined with the gate port terminated in the complex conjugate of the MESFET's input impedance, thereby satisfying the matching condition. The ratio m , the mixed signal component V_{mix} , and the input signal component V_{sig} contained in the MESFET output signal, can be calculated by the method shown in the Appendix. Two examples are shown in Figs. 8 and 9. Fig. 8 shows how m , V_{mix} , and V_{sig} change with varying gate bias V_0 . It is shown that as m approaches unity with increasing V_0 the conversion loss, V_{mix} , increases. Therefore, the gate bias must be set at a slightly higher voltage than that which gives the minimum loss, say $V_0 = 0.4 \text{ V}$. Fig. 9 shows the change of m , V_{mix} , and V_{sig} when the local-oscillator voltage V_1 is varied. It is shown that V_1 affects m similarly to the manner V_0 does.

IV. MESFET REGENERATOR EXPERIMENTAL RESULTS

Fig. 10 shows an experimental FET mixer circuit for a signal frequency of 1.7 GHz. A 3-dB hybrid is used to separate the local oscillator from the input signal. The FET used here is an n-channel GaAs MESFET (2SK85) developed for X-band low-noise amplifiers or oscillators. The output filter is a fifth-order Chebyshev-type low-pass filter with

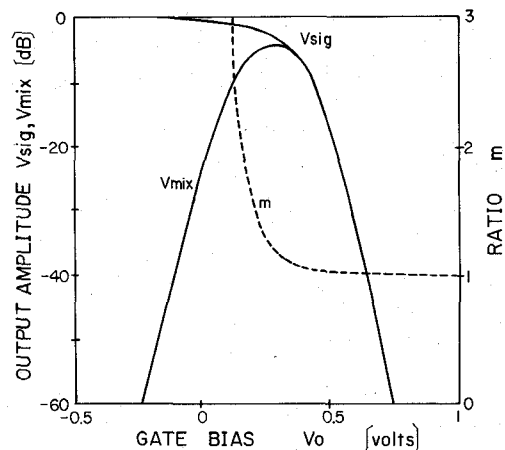
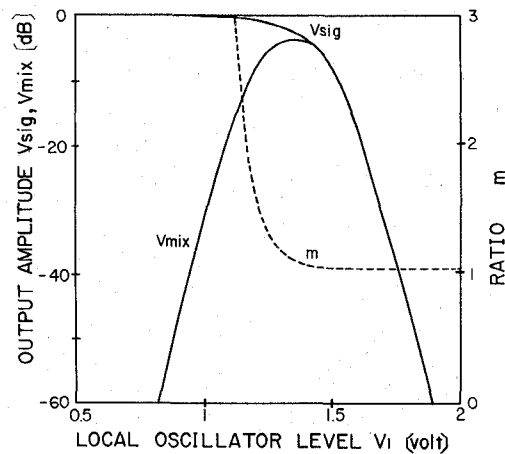
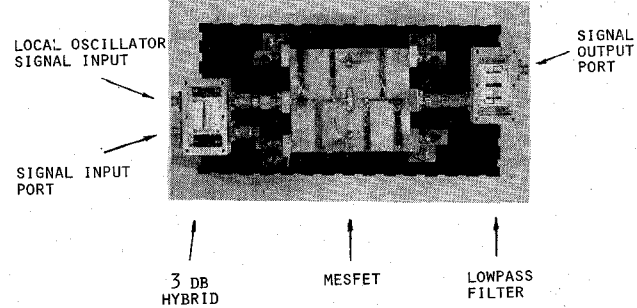
Fig. 8. Ratio m and output signal voltages V_{sig} , V_{mix} versus gate bias voltage. (Local-oscillator signal voltage $V_1 = 1 \text{ V}$.)Fig. 9. Ratio m and output signal voltages V_{sig} , V_{mix} versus local oscillator level. (Gate bias voltage $V_0 = 0 \text{ V}$.)

Fig. 10. Experimental MESFET mixer circuit.

1.8-GHz cutoff frequency. Fig. 11 shows the direct regenerator measurement circuit. The carrier frequency is 1.7 GHz and the modulating signal is ninth-order pseudo random noise, with a speed of 20 Mbits/s. A tunnel diode is used for the limiter, but any limiter can be used, provided that the AM-PM conversion is suppressed.

In order to measure the ratio m , a spectrum analyzer and a 3.4-GHz incoherent local oscillator are used, together with the unmodulated 1.7-GHz signal. A network analyzer is used to measure the input-output phase characteristics of the regenerator, with a phase shifter replacing the modulator.

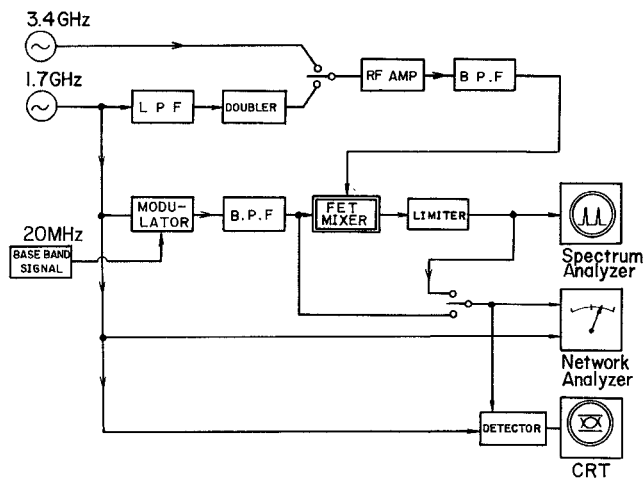
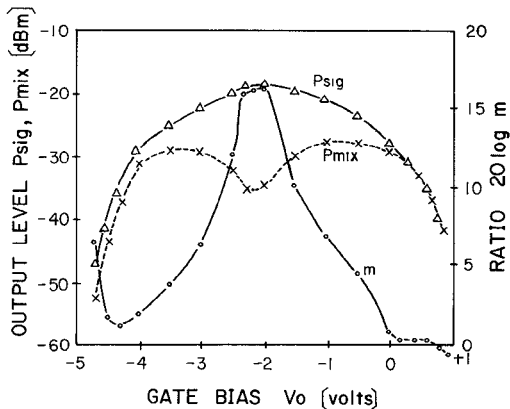
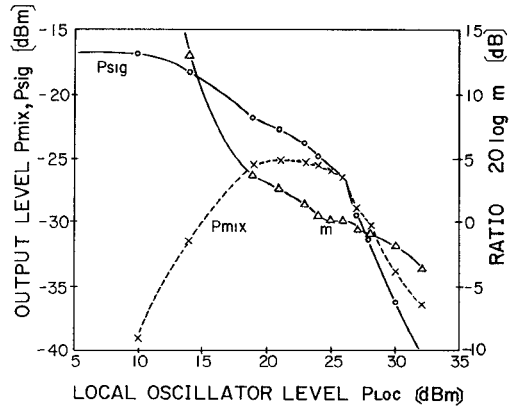


Fig. 11. Measurement circuits for the phase regenerator.

Fig. 12. Measured ratio m and output signal levels P_{sig} , P_{mix} versus gate bias voltage. (Input signal $P_{\text{in}} = -15$ dBm; local-oscillator power $P_{\text{loc}} = +10$ dBm.)Fig. 13. Measured ratio m and output signal levels P_{sig} , P_{mix} versus local-oscillator level. (Input signal $P_{\text{in}} = -15$ dBm; gate bias voltage $V_0 = 0$ V.)

A coherent phase detector and a CRT are used to measure the vector locus or the eye diagrams.

Fig. 12 shows measured values for m versus gate bias voltage. Fig. 13 shows m versus local-oscillator level. In the same graphs P_{mix} and P_{sig} are shown, which express the mixed signal component and the input signal component at the output, respectively. Fig. 12 shows that mixing is

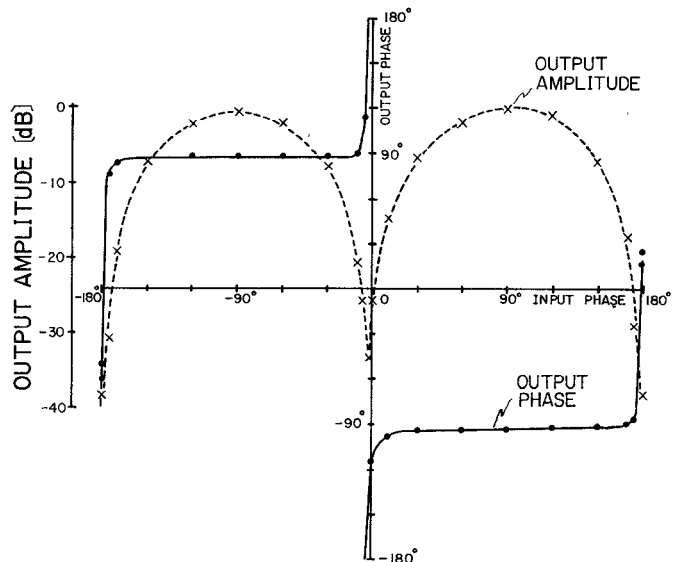


Fig. 14. Measured input-output phase and amplitude characteristic versus input phase.

performed both in the pinch-off region and the Schottky region. The ratio m is about unity ($m = 0$ dB) at $V_0 \geq 0.2$ V, and is less than unity at $V_0 \geq 0.8$ V. Fig. 13 shows that the local-oscillator level P_{loc} has a similar effect as the gate bias V_0 . These figures agree with the theoretical predictions, except for the mixing effect in the pinch-off region. The existence of the region $m \leq 1$ may be caused by signal reflections between the gate and the local-oscillator port. Excess loss may be caused in part by the circuits, such as mismatch at the drain or local-oscillator port.

The solid line in Fig. 14 shows measured input versus output phase characteristics. These results show that the static phase characteristic is step-like and that almost perfect regeneration in phase can be obtained. As the input signal phase is varied by the phase shifter, the phase angle is measured under noise-free conditions. The broken line in Fig. 14 shows the measured input-phase versus output-amplitude characteristic. These results agree with the theoretical predictions presented in Fig. 4.

The measured dynamic performance is shown in Fig. 15 and eye diagrams are shown in Fig. 16. The input signal is band limited by the RF bandpass filter, so the input signal suffers both amplitude and phase modulations, which distort the transient and results in intersymbol interference. Fig. 15(a) clearly shows these amplitude and phase modulations. If this input signal is applied to the limiter, AM is suppressed, but PM is not suppressed. Fig. 15(b) shows the limiter operation clearly. Fig. 15(c) shows the vector locus of the direct regenerator output signal. In this regenerator, constructed of a MESFET phase regenerator and a limiter, AM and PM are suppressed. Fig. 15(d) shows the direct regenerator output without limiter. It is shown that PM is suppressed, but AM is not suppressed. These results show that the MESFET phase regenerator can suppress PM and the limiter suppresses the AM, even in dynamic operation.

Fig. 16(a) shows the eye diagram of the input signal. The rise time is large and is caused by the RF band limita-

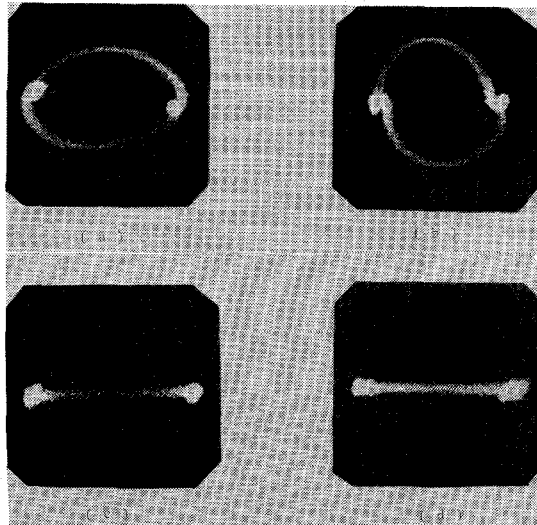


Fig. 15. Transient vector locus. (a) Direct regenerator input signal. (b) Output signal of the direct regenerator without the MESFET regenerator. (c) Direct regenerator output signal. (d) Output signal of the direct regenerator without the limiter.

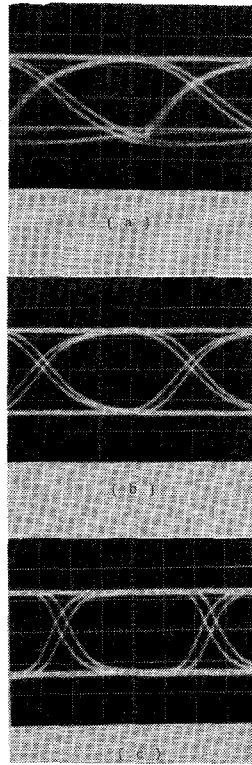


Fig. 16. Eye diagrams. (a) Direct regenerator input signal. (b) Output signal of the direct regenerator without the MESFET phase regenerator. (c) Direct regenerator output signal. (Horizontal scale: 10 ns/div.)

tion. Fig. 16(b) shows the limiter output. Now the rise time is shortened as a result of the AM suppression. Fig. 16(c) shows the direct regenerator output. The regenerator improves the rise time even more compared with that shown in Fig. 15(b), because both AM and PM are suppressed. These results show that waveform regeneration can be performed by suppressing AM and PM. In the same manner, AM and PM fluctuations caused by noise may be suppressed using this regenerator.

Fig. 17 shows the Lissajou figures for various cases. These figures show that there is no phase error for the various cases.

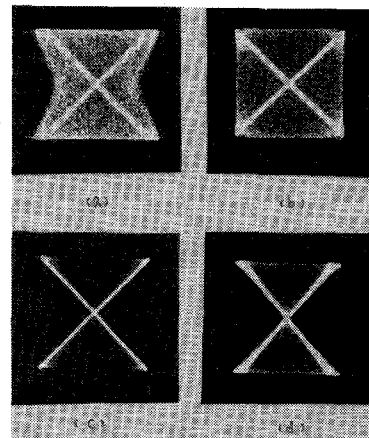


Fig. 17. Lissajou figures. (a) Direct regenerator input signal. (b) Output signal of the direct regenerator without the MESFET regenerator. (c) Direct regenerator output signal. (d) Output signal of the direct regenerator without the limiter. (Horizontal input: signal to be measured. Vertical input: reference carrier.)

V. CONCLUSION

This paper proposes a direct regenerator at the carrier frequency using a GaAs MESFET, which results in a circuit that simplifies the separation of the input port from the output port. Static and dynamic phase-regeneration characteristics have been measured, using the experimental MESFET regenerator. Results show that the regenerator performance depends mainly on gate bias voltage and local-oscillator level, as predicted by the analysis. By adjusting these parameters, good performance is obtained for a 1.7-GHz signal with 20-Mbits/s modulation frequency. This MESFET regenerator is relatively narrow-band at both input and output ports. However, the signal speed of the regenerator will be higher than 200 Mbits/s if the input and output circuits are matched over a wider frequency range.

APPENDIX

From Fig. 7, the impedance matrix (Z) at the gate port is obtained as

$$\begin{aligned} \begin{bmatrix} V_{G\text{sig}} \\ V_{G\text{mix}} \end{bmatrix} &= \begin{bmatrix} R & 0 \\ 0 & R \end{bmatrix} \begin{bmatrix} I_{G\text{sig}} \\ I_{G\text{mix}} \end{bmatrix} + \begin{bmatrix} V_{J\text{sig}} \\ V_{J\text{mix}} \end{bmatrix} \\ &= \begin{bmatrix} R & 0 \\ 0 & R \end{bmatrix} \begin{bmatrix} I_{G\text{sig}} \\ I_{G\text{mix}} \end{bmatrix} + \begin{bmatrix} j\omega C & 0 \\ 0 & j\omega C \end{bmatrix} \\ &\quad + \begin{bmatrix} g_0 & g_1 \\ g_1 & g_0 \end{bmatrix}^{-1} \begin{bmatrix} I_{G\text{sig}} \\ I_{G\text{mix}} \end{bmatrix} \\ &= (Z) \begin{bmatrix} I_{G\text{sig}} \\ I_{G\text{mix}} \end{bmatrix} \end{aligned} \quad (A.1)$$

where

$$\begin{aligned} (Z) &= \begin{bmatrix} Z_{11} & Z_{12} \\ Z_{21} & Z_{22} \end{bmatrix} \\ &= \begin{bmatrix} R & 0 \\ 0 & R \end{bmatrix} + \begin{bmatrix} j\omega C & 0 \\ 0 & j\omega C \end{bmatrix} + \begin{bmatrix} g_0 & g_1 \\ g_1 & g_0 \end{bmatrix}^{-1} \end{aligned} \quad (A.2)$$

g_0, g_1 are the conversion conductances, and

$$\begin{aligned} g_0 &= \alpha I_s \exp(\alpha V_0) \cdot I_0(\alpha V_1) \\ g_1 &= \alpha I_s \exp(\alpha V_0) \cdot I_1(\alpha V_1) \end{aligned} \quad (A.3)$$

with $I_m(\cdot)$ the modified Bessel functions of order m . If the mixed signal is assumed to be terminated by Z_L

$$V_{G\text{mix}} = -Z_L I_{G\text{mix}}. \quad (\text{A.4})$$

From (A.1) and (A.4), a relation between $V_{G\text{sig}}$ and $V_{G\text{mix}}$ is obtained

$$V_{G\text{mix}} = k_1 V_{G\text{sig}} \quad (\text{A.5})$$

where

$$k_1 = Z_{21}Z_L/(Z_{11}Z_L - Z_{12}Z_{21} + Z_{22}Z_{11}). \quad (\text{A.6})$$

On the other hand, the relation between the gate voltage and the junction voltage is

$$\begin{aligned} \begin{bmatrix} V_{G\text{sig}} \\ V_{G\text{mix}} \end{bmatrix} &= \begin{bmatrix} R & 0 \\ 0 & R \end{bmatrix} \cdot \begin{bmatrix} I_{G\text{sig}} \\ I_{G\text{mix}} \end{bmatrix} + \begin{bmatrix} V_{J\text{sig}} \\ V_{J\text{mix}} \end{bmatrix} \\ &= \begin{bmatrix} R & 0 \\ 0 & R \end{bmatrix} \cdot \begin{bmatrix} [i\omega C & 0] \\ [0 & j\omega C] \end{bmatrix} + \begin{bmatrix} g_0 & g_1 \\ g_1 & g_0 \end{bmatrix} \\ &\quad + \begin{bmatrix} 1 & 0 \\ 0 & 1 \end{bmatrix} \cdot \begin{bmatrix} V_{J\text{sig}} \\ V_{J\text{mix}} \end{bmatrix}. \end{aligned} \quad (\text{A.7})$$

Therefore

$$\begin{bmatrix} V_{J\text{sig}} \\ V_{J\text{mix}} \end{bmatrix} = (K) \cdot \begin{bmatrix} V_{G\text{sig}} \\ V_{G\text{mix}} \end{bmatrix} \quad (\text{A.8})$$

where

$$\begin{aligned} (K) &= \begin{bmatrix} K_{11} & K_{12} \\ K_{21} & K_{22} \end{bmatrix} \\ &= \begin{bmatrix} R & 0 \\ 0 & R \end{bmatrix} \begin{bmatrix} [i\omega C & 0] \\ [0 & j\omega C] \end{bmatrix} + \begin{bmatrix} g_0 & g_1 \\ g_1 & g_0 \end{bmatrix} \\ &\quad + \begin{bmatrix} 1 & 0 \\ 0 & 1 \end{bmatrix}^{-1}. \end{aligned} \quad (\text{A.9})$$

From (A.5) and (A.8), the mixed signal and the input signal voltage at the junction are obtained as

$$\begin{bmatrix} V_{J\text{sig}} \\ V_{J\text{mix}} \end{bmatrix} = \begin{bmatrix} K_{11} & K_{12} \cdot k_1 \\ K_{21} & K_{22} \cdot k_1 \end{bmatrix} \begin{bmatrix} V_{G\text{sig}} \\ V_{G\text{mix}} \end{bmatrix}. \quad (\text{A.10})$$

It is clear that the MESFET output signal is determined by the junction voltage. Therefore, the output signal normalized to $V_{G\text{sig}}$ is

$$\begin{aligned} V_{\text{sig}} &= |V_{J\text{sig}}|/|V_{G\text{sig}}| = |K_{11} + K_{12}k_1| \\ V_{\text{mix}} &= |V_{J\text{mix}}|/|V_{G\text{sig}}| = |K_{21} + K_{22}k_1|. \end{aligned} \quad (\text{A.11})$$

The ratio m , which is defined by (9), is

$$\begin{aligned} m &= V_{\text{sig}}/V_{\text{mix}} \\ &= |K_{11} + K_{12}k_1|/|K_{21} + K_{22}k_1|. \end{aligned} \quad (\text{A.12})$$

ACKNOWLEDGMENT

The authors wish to thank Y. Nakamura and members of NTT's Electrical Communication Laboratories for their guidance, encouragement, and cooperation in the course of this study.

REFERENCES

- [1] H. Fuketa and T. Kurosaki, "Experimental studies on phase regeneration method in carrier stage of a 4-phase PM system," *Trans. Inst. Electronics Comm. Eng. Japan*, vol. 49, no. 10, pp. 1835-42, Oct. 1966.
- [2] S. Ohwaku, M. Hata, and N. Kondo, "Experiments on direct regeneration of PCM phase modulated signal," *Trans. Inst. Electronics Comm. Eng. Japan*, vol. 49, no. 11, pp. 2217-24, Nov. 1966.
- [3] M. Hata *et al.*, "A new phase coherent parametric mixer for PCM-PSK communications," *G-MTT*, 1972.
- [4] T. Ohta and M. Hata, "Parametric amplifier having phase regenerative effect," *Trans. Inst. Electronics Comm. Eng. Japan*, vol. 53-B, no. 4, pp. 202-209, April 1970.
- [5] O. Kurita and K. Morita, "Microwave MESFET mixer," this issue, pp. 361-366.

Short Papers

Submicrometer Self-Aligned GaAs MESFET

P. BAUDET, M. BINET, AND D. BOCCON-GIBOD

Abstract—This short paper presents a self-aligned technique which permits the production of submicrometer gate lengths and spacings between contacts. The exclusive use of standard photolithographic techniques makes this method interesting. Microwave measurements are reported for such a device with a 0.7- μm gate length in a 2.2- μm drain-source spacing. The yield of the process is usually better than 80 percent.

INTRODUCTION

Since 1968 the improvement of the GaAs MESFET has required the use of smaller and more refined geometries. Thus alignment rapidly became one of the major problems in the process. To solve this difficulty, several laboratories have proposed various self-aligned methods [1]-[3]. But except for Middelhoek [4], nobody, to our knowledge, has published a self-aligned method which allows the realization of submicrometer gate and spacing contact lengths. The purpose of this short paper is to describe a new and simple method of self-alignment which does not necessitate the use of electron-beam technology.

Whereas the other methods generally use self-alignment from source and drain contacts by using the undercutting or over-